Soil Inorganic Carbon Sequestration Following Afforestation Is Probably Induced by Pedogenic Carbonate Formation in Northwest China

Yang Gao[1,2], Jing Tian[2], Yue Pang[2] and Jiabin Liu[1,3]*

[1] State Key Laboratory of Soil Erosion and Dryland Farming on the Loess Plateau, Northwest A&F University, Yangling, China, [2] College of Forestry, Northwest A&F University, Yangling, China, [3] College of Natural Resources and Environment, Northwest A&F University, Yangling, China

In arid and semiarid areas, the effects of afforestation on soil organic carbon (SOC) have received considerable attention. In these areas, in fact, soil inorganic carbon (SIC), rather than SOC, is the dominant form of carbon, with a reservoir approximately 2–10 times larger than that of SOC. A subtle fluctuation of SIC pool can strongly alter the regional carbon budget. However, few studies have focused on the variations in SIC, or have used stable soil carbon isotopes to analyze the reason for SIC variations following afforestation in degraded semiarid lands. In the Mu Us Desert, northwest China, we selected a shifting sand land (SL) and three nearby forestlands (Populus alba) with ages of 8 (P-8), 20 (P-20) and 30 (P-30) years, and measured SIC, SOC, soil organic and inorganic $\delta^{13}C$ values ($\delta^{13}C$-SOC and $\delta^{13}C$-SIC) and other soil properties. The results showed that SIC stock at 0–100 cm in SL was 34.2 Mg ha^{-1}, and it increased significantly to 42.5, 49.2, and 68.3 Mg ha^{-1} in P-8, P-20, and P-30 lands, respectively. Both $\delta^{13}C$-SIC and $\delta^{13}C$-SOC within the 0–100 cm soil layer in the three forestlands were more negative than those in SL, and gradually decreased with plantation age. Afforestation elevated soil fine particles only at a depth of 0–40 cm. The entire dataset (260 soil samples) exhibited a negative correlation between $\delta^{13}C$-SIC and SIC content ($R^2 = 0.71$, $P < 0.01$), whereas it showed positive correlation between SOC content and SIC content ($R^2 = 0.52$, $P < 0.01$) and between $\delta^{13}C$-SOC and $\delta^{13}C$-SIC ($R^2 = 0.63$, $P < 0.01$). However, no correlation was observed between SIC content and soil fine particles. The results indicated that afforestation on shifting SL has a high potential to sequester SIC in degraded semiarid regions. The contribution of soil fine particle deposition by canopy to SIC sequestration is limited. The SIC sequestration following afforestation is very probably caused by pedogenic carbonate formation, which is closely related to SOC accumulation. Our findings suggest that SIC plays an important role in the carbon cycle in semiarid areas and that overlooking this carbon pool may substantially lead to underestimating carbon sequestration capacity following vegetation rehabilitation.

Keywords: afforestation, degraded semiarid regions, pedogenic inorganic carbon, soil inorganic carbon, stable carbon isotope

INTRODUCTION

Arid and semiarid areas cover approximately 41% of the Earth's land surface (Reynolds et al., 2007; Delgado-Baquerizo et al., 2013). In these areas, desertification is an extremely challenging environmental problem leading to serious land degradation and enormous losses of soil carbon (Lal, 2009; Li et al., 2015). However, if appropriate restoration measures can be successfully implemented on degraded lands, it is possible to effectively curb land degradation and substantially improve the soil properties in these lands (Lal, 2004; Huang et al., 2012). Afforestation is an important restoration measure for degraded lands and is generally considered to have great potential to combat desertification, protect soils and alter the soil carbon pool (Lal, 2010). The soil carbon pool comprises the soil organic carbon (SOC) and soil inorganic carbon (SIC) pools (Zhang et al., 2015). Because of its potentially rapid response to afforestation, the SOC pool has received considerable attention and has been extensively investigated (Jackson et al., 2002; Deng et al., 2014). In contrast to the great progress made in understanding the dynamics of the SOC pool, the effects of afforestation on the SIC pool have received relatively less consideration (Wang et al., 2010; Meyer et al., 2014). In fact, SIC, rather than SOC, is the dominant form of carbon in arid and semiarid areas (Mielnick et al., 2005; Mi et al., 2008), with a reservoir approximately 2–10 times larger than that of SOC (Schlesinger, 1982; Tan et al., 2014). Due to the large reservoir of SIC, a subtle fluctuation in the SIC pool will strongly alter the carbon budget in arid and semiarid areas (Landi et al., 2003; Jin et al., 2014). It is therefore important to have a thorough understanding of the dynamics of SIC pool following afforestation in these regions.

Changes in SIC following afforestation in arid and semiarid areas exhibit contrasting trends, some of which are in direct opposition. For instance, in the Horqin Sandy Land and Badain Jaran Desert, China, planting Mongolian pine and poplar significantly stimulated the accumulation of SIC (Su et al., 2010; Li Y.Q. et al., 2013). In contrast, in the Columbia Plateau of Oregon, United States, poplar afforestation was found to reduce the SIC stock (Sartori et al., 2007). Another study in the Loess Plateau of China reported that afforestation simply redistributed SIC along the soil profile without affecting its total quantity (Chang et al., 2012). These results indicate that the effects of afforestation on SIC stock need to be further examined in arid and semiarid areas.

Importantly, uncertainty nonetheless remains as to why SIC showed variation following afforestation. There are several geological methods (such as scanning electron microscopes) for studying SIC variations (Zamanian et al., 2016). Among these, stable soil carbon isotopes (^{13}C) have been demonstrated to be an applicable and crucial indicator revealing the reason for SIC variations following land use changes (Cerling et al., 1989; Stevenson et al., 2005). The SIC pool consists of lithogenic inorganic carbon (LIC) and pedogenic inorganic carbon (PIC) pools, and these two subpools have different δ^{13}C values (Jobbágy and Jackson, 2003; Chang et al., 2012; Tan et al., 2014).

The LIC subpool is inherited from the parent material and generally has high δ^{13}C values (close to zero), whereas the PIC subpool is generated from the precipitation of carbonate ions and generally shows low δ^{13}C values (negative) (Wang et al., 2016; Zamanian et al., 2016). The dynamics of the SIC pool following land use changes are dominated by the LIC and PIC subpools. Various processes in SIC variations, including the mixing of LIC with PIC and the reaction of soil carbonate with biogenic CO_2, can be sensitively and precisely reflected in δ^{13}C values (Stevenson et al., 2005; Monger et al., 2015). The use of stable soil carbon isotopes method, in which the soil inorganic δ^{13}C value (δ^{13}C-SIC) and the soil organic δ^{13}C value (δ^{13}C-SOC) are measured, has been found to be an ideal approach to studying the inherent mechanisms of SIC dissolution, sequestration and transformation following land use changes (Stevenson et al., 2005; Rao et al., 2006; Li G.J. et al., 2013; Wang J.P. et al., 2015). In arid croplands, determining the changes in δ^{13}C-SIC and δ^{13}C-SOC following straw organic amendments, revealed that such amendments enhanced PIC formation and led to SIC accumulation (Wang et al., 2014; Wang X.J. et al., 2015). In semiarid restored grassland, a decrease in δ^{13}C-SIC indicated that soil carbonate exchanged with biogenic CO_2, resulting in lower SIC stock in grassland than in farmland (Liu et al., 2014). Despite the value provided by the existing carbon isotope methods, they have not been extensively utilized to explore the reason for SIC variations after afforestation in degraded semiarid lands, particularly for afforestation on shifting sand land (SL).

Sand land, which is widely distributed in northwest China, is characterized by extreme deterioration of the plant and soil environment. Afforestation and shrub-planting are commonly suggested as options to combat desertification (Zhang K. et al., 2010; Zhang Y. et al., 2013). Previous studies have conclusively demonstrated that afforestation on SL significantly promotes SOC storage (Liu et al., 2013; Li et al., 2016). However, few studies have focused on the variations in SIC, or have used stable soil carbon isotopes to analyze the mechanisms underlying SIC variations following afforestation on SL. The use of the related field data along a chronosequence of afforestation, which could more precisely and reliably determine the dynamics of SIC, has rarely been reported. The changes in soil carbon along a chronosequence of afforestation are often studied by comparing the different-aged forestlands within a designated area (space-for-time substitution approach) (Farley et al., 2004; Qiu et al., 2015), as the historical data in a same forestland since the beginning of afforestation cannot be obtained at present. In view of the above deficiencies, we selected an SL and three nearby forestlands (*Populus alba*) with ages of 8 (P-8), 20 (P-20), and 30 (P-30) years within 2 km^2 in the Mu Us Desert, northwest China. We measured SIC, SOC, δ^{13}C-SOC and δ^{13}C-SIC in both the SL and the three different-aged forestlands at depth of 100 cm. The objectives of this research were (1) to examine the changes in SIC along a chronosequence of afforestation and (2) to explore the reasons for SIC variations following afforestation using the carbon isotope method.

FIGURE 1 | Distribution of the four sample plots in the study area and the relationships between sample plot, subplot and hole. The satellite image was obtained from Google Earth and was taken in January 2013. Other pictures were taken by YG in September 2015.

MATERIALS AND METHODS

Study Site Description

The study site is located at the Station of Chunlan Bai Desertification Control, Yanchi County, Ningxia Province, China (107°27′ E, 37°54′ N), on the southwestern edge of the Mu Us Desert. The region has a typical temperate continental monsoon climate with an elevation of 1308 m. The mean annual precipitation is 275 mm, with 73% occurring in summer and autumn. The mean annual temperature is 7°C. The average relative humidity is 51% and the frost-free period lasts for 128 days. According to the US Soil Taxonomy system, the soil type is quartisamment (Gao et al., 2014), with a pH range of 8.0 to 9.0. In the 1980s, the landscape of the research area was dominated by SL, which comprised many connected active sand dunes devoid of any vegetation. At that time, the groundwater level was high enough (2 m) to supply water for tree growth. Afforestation with poplar (*Populus alba*) on SL was successively performed by Chunlan Bai and her family to restrict sand movement and to protect their homeland. At present, forestlands with different plantation ages have been established at the study site. Additionally, areas of SL at some distance from human habitation have not been managed, and have remained active. Previous studies have confirmed that the soil properties in the SL do not vary over a prolonged period of time (Su and Zhao, 2003; Su et al., 2010), suggesting that the soil properties prior to the start of the experiments can be represented by those in the SL at the time of the study. Therefore, the present-day SL can be used as a control for investigating the changes in SIC and soil stable carbon isotopes following afforestation. In this study, we used different-aged forestlands to explore the dynamics of SIC along a chronosequence of

afforestation, because there had been no related study in this region and there was a lack of historical data. Within the scope of the 2 km × 1 km in the study site, we selected an SL and its nearby three different-aged forestlands as the four treatments: (1) the SL (control), (2) an 8-year-old poplar land, (3) a 20-year-old poplar land, and (4) a 30-year-old poplar land. For each treatment, we selected one sample plot. The distribution of the four sample plots within the study site is illustrated in **Figure 1**, and information on the four sample plots is presented in **Table 1**.

Soil Sampling and Analyses

Thirteen 20 m × 20 m subplots were randomly selected within each sample plot for soil sampling. In each subplot, five holes (100 cm in depth) along an S-shaped curve were drilled using a soil auger (10 cm in diameter) after removing litter (the relationships between sample plot, subplot and hole are shown in **Figure 1**). The soil samples were obtained at a depth interval of 20 cm from 0 to 100 cm. In each subplot, five soil samples obtained from five holes at the same layer were mixed into a composite sample (approximately 500 g), and five composite samples were achieved at a depth interval of 20 cm from 0 to 100 cm within each subplot. Sixty-five composite samples from the 13 subplots within each sample plot were obtained. After the samples were air-dried, roots were removed from all the 260 composite samples from the four sample plots. For each air-dried composite sample, approximately 50 g soil was taken and retained for measuring particle size distribution using a particle size analyzer (Malven Laser Mastersizer 2000, England). The remaining air-dried composite samples were fully ground in an agate mortar and passed through a 0.1 mm sieve for SIC content, SOC content and soil $\delta^{13}C$ analyses.

TABLE 1 | Characteristics of the four sample plots (mean ± standard deviation; $n = 13$).

Plots	Unit	SL	P-8	P-20	P-30
Sample plot area	ha	4	3	3	3
Plant species		–	*Populus alba*	*Populus alba*	*Populus alba*
Density	trees ha^{-1}	0	585	543	502
Height	m	0	6.4 ± 1.1	12.8 ± 2.2	15.5 ± 2.7
Diameter at breast height	cm	0	6.2 ± 0.8	15.8 ± 1.9	22.6 ± 2.7
Coverage	%	0	28.9	35.7	40.2
Soil electrical conductivity	dS m^{-1}	4.52 ± 0.37	4.73 ± 0.26	4.68 ± 0.24	4.86 ± 0.38
Ca^{2+} in soil	cmol kg^{-1}	4.79 ± 0.24	4.68 ± 0.35	4.92 ± 0.21	5.01 ± 0.18
Mg^{2+} in soil	cmol kg^{-1}	0.33 ± 0.08	0.41 ± 0.04	0.39 ± 0.05	0.48 ± 0.05
Soil total porosity	%	40.3 ± 0.8	43.5 ± 0.7	44.6 ± 0.5	45.7 ± 0.7

After obtaining the 260 composite samples, a soil profile at 0–100 cm was excavated within each subplot. A metal corer (100 cm^3 in volume) was driven into the soil at a depth interval of 20 cm from 0 to 100 cm, and then soil samples were oven dried at 115°C for 24 h and weighed to determine bulk density. From the excavated soil profile in each subplot, additional soil samples were obtained at a depth interval of 20 cm from 0 to 100 cm for measuring Soil pH, using a 2.5:1 ratio of deionized water/soil mass. SOC content was determined using the dichromate oxidation procedure described by Walkley and Black (1934). SIC content was determined using the pressure calcimeter method (Wang et al., 2012). The stocks of SIC were calculated as follows:

$$M = 0.1 \times D \times B \times Z \times ((100 - G)/100) \quad (1)$$

where M is soil carbon stock per unit area (Mg ha^{-1}); D is soil depth (cm); B is bulk density (g cm^{-3}); Z is carbon content (g kg^{-1}) and G is the relative amount of gravel (%). The gravel content was 0 because there was no gravel in the soil.

The detailed methods for determining δ^{13}C-SOC and δ^{13}C-SIC have been described previously by Jin et al. (2014). For the determination of δ^{13}C-SOC, 5 g of ground and sieved soil was steeped in 2 M HCl for 24 h to remove SIC. The treated soil was then washed with distilled water until the pH exceeded 5, and was subsequently dried at 40°C. From each dried soil sample, approximately 30 mg soil was packed in a tin cup and analyzed with an elemental analyzer (Flash EA 1112, Thermo Fisher Scientific, Inc.) and an isotope ratio mass spectrometer (IRMS) (Finnigan MAT Delta plus XP, Thermo Fisher Scientific, Inc.). The contents of the tin cup were combusted at 1000°C in the EA, and then the SOC of the sample in the tin cup was converted to CO$_2$. The CO$_2$ from the EA was ionized and its δ^{13}C value was measured by IRMS. The working standards used for determining δ^{13}C-SOC were Protein (Elemental Analyses, Inc., Beijing, China, −26.98‰) and NBS-19 (National Institute of Standards and Technology, Gaithersburg, MD, United States; +1.95‰).

To determine ^{13}C-SIC, approximately 100 mg sieved soil was reacted with 5 mL 100% H$_3$PO$_4$ for 2 h at 75°C in a 12 mL sealed vessel of Gas Bench II (Thermo Fisher Scientific, Inc.) to generate CO$_2$, and the generated CO$_2$ was measured by IRMS (Finnigan MAT Delta plus XP, Thermo Fisher Scientific,

Inc.). The working standards used for determining δ^{13}C-SIC were NBS-18 (National Institute of Standards and Technology, Gaithersburg, MD, United States; −5.01‰) and NBS-19.

The stable isotope compositions of the SOC and SIC, expressed in delta (δ) notation, were both calculated as follows (Coplen, 2011):

$$\delta^{13}C = \frac{(^{13}C/^{12}C)_{sample}}{(^{13}C/^{12}C)_{standard}} - 1 \quad (2)$$

where $(^{13}C/^{12}C)_{sample}$ and $(^{13}C/^{12}C)_{standard}$ are the atomic ratio of ^{13}C to ^{12}C in the sample and in the Vienna Pee Dee Belemnite (VPDB) standard, respectively. All samples were measured in triplicate. In the three measurements for each sample, the standard deviation of the reported δ^{13}C-SOC and δ^{13}C-SIC in this study was within 0.4 and 0.3‰, respectively.

Statistical Analyses

Statistical analyses were performed using version 16.0 of the SPSS software (SPSS, Chicago, IL, United States). Two-way analysis of variance was conducted to test the effects of soil depth and plant age, as well as their interactions with soil carbon contents and soil δ^{13}C values (**Table 2**). Multiple comparisons and one-way analysis of variance procedures were used to compare the differences in soil carbon contents and soil δ^{13}C values between different treatments within the same depth, and between different soil depths within the same treatment. Mean comparisons were performed using the least-significant-difference test. Linear regression analyses were carried out to evaluate the relationships between various carbon variables (SOC vs. SIC, δ^{13}C-SIC vs. SIC, δ^{13}C-SIC vs. δ^{13}C-SOC, SIC vs. silt particle, SIC vs. clay particle).

RESULTS

Bulk Density, Soil Particle Content and pH in Shifting Sand Land and Forestlands

Afforestation was found to cause a variation in bulk density and fine particles at 0–40 cm soil layer (**Table 3**). Within this depth, the bulk densities in P-20 land and P-30 land were significantly lower than in SL, but there was no significant difference between

TABLE 2 | Two-way ANOVA for soil carbon content, δ^{13}C-SIC, and δ^{13}C-SOC in for treatments and soil layers.

Soil carbon	Treatment		Layer		Treatment × Layer	
	F	P	F	P	F	P
SOC	935.7	<0.001	39.78	<0.001	7.1	<0.001
SIC	156.86	<0.001	2.27	0.062	1.82	0.046
δ^{13}C-SIC	217.19	<0.001	1.81	0.128	0.31	0.986
δ^{13}C-SOC	150.57	<0.001	6.45	<0.001	1.22	0.267

TABLE 3 | Bulk density, particle content and pH of soil in the four sample plots ($n = 13$, mean ± SD).

Soil properties	Soil depth (cm)	SL	P-8	P-20	P-30
Bulk density (g cm^{-3})	0–20	1.58 ± 0.14 a	1.51 ± 0.14 ab	1.45 ± 0.09 bc	1.43 ± 0.13 c
	20–40	1.56 ± 0.11 a	1.54 ± 0.11 ab	1.47 ± 0.15 bc	1.45 ± 0.14 c
	40–60	1.57 ± 0.13 a	1.52 ± 0.10 a	1.51 ± 0.12 a	1.49 ± 0.11 a
	60–80	1.59 ± 0.12 a	1.56 ± 0.13 a	1.55 ± 0.16 a	1.54 ± 0.09 a
	80–100	1.57 ± 0.09 a	1.58 ± 0.12 a	1.53 ± 0.13 a	1.52 ± 0.14 a
Sand (>0.05 mm, %)	0–20	91.3 ± 3.5 a	90.0 ± 3.8 a	89.7 ± 3.9 a	89.2 ± 2.9 a
	20–40	91.7 ± 2.6 a	90.7 ± 2.4 a	90.5 ± 2.8 a	90.9 ± 3.2 a
	40–60	91.9 ± 2.1 a	91.7 ± 3.2 a	91.1 ± 2.1 a	91.5 ± 3.4 a
	60–80	92.2 ± 3.2 a	91.9 ± 2.9 a	91.7 ± 3.6 a	91.6 ± 3.8 a
	80–100	92.6 ± 3.3 a	92.1 ± 2.8 a	92.6 ± 2.7 a	92.7 ± 3.9 a
Silt (0.002–0.05 mm, %)	0–20	4.8 ± 0.3 b	5.3 ± 0.4 a	5.4 ± 0.3 a	5.8 ± 0.3 a
	20–40	4.7 ± 0.2 b	5.1 ± 0.4 ab	5.0 ± 0.3 ab	5.2 ± 0.5 a
	40–60	4.9 ± 0.3 a	4.8 ± 0.3 a	5.1 ± 0.4 a	4.9 ± 0.3 a
	60–80	4.6 ± 0.2 a	4.9 ± 0.5 a	4.8 ± 0.4 a	4.7 ± 0.3 a
	80–100	4.7 ± 0.4 a	4.8 ± 0.2 a	4.6 ± 0.3 a	4.9 ± 0.4 a
Clay (<0.002 mm, %)	0–20	3.9 ± 0.4 b	4.7 ± 0.3 a	4.9 ± 0.2 a	5.0 ± 0.4 a
	20–40	3.6 ± 0.5 b	4.2 ± 0.4 ab	4.5 ± 0.5 a	3.9 ± 0.3 ab
	40–60	3.2 ± 0.6 a	3.5 ± 0.3 a	3.8 ± 0.5 a	3.6 ± 0.5 a
	60–80	3.2 ± 0.4 a	3.2 ± 0.3 a	3.5 ± 0.3 a	3.7 ± 0.4 a
	80–100	2.7 ± 0.5 a	3.1 ± 0.4 a	2.8 ± 0.4 a	2.4 ± 0.3 a
pH	0–20	8.9 ± 0.3 a	8.6 ± 0.4 ab	8.2 ± 0.3 b	8.1 ± 0.2 b
	20–40	9.0 ± 0.3 a	8.5 ± 0.3 b	8.2 ± 0.2 bc	8.0 ± 0.3 c
	40–60	8.8 ± 0.2 a	8.3 ± 0.4 ab	8.1 ± 0.1 ab	7.9 ± 0.2 b
	60–80	8.7 ± 0.1 a	8.4 ± 0.2 ab	8.2 ± 0.3 b	8.2 ± 0.1 b
	80–100	8.9 ± 0.2 a	8.5 ± 0.3 ab	8.3 ± 0.4 b	8.1 ± 0.3 b

Within each depth, different lowercase letters denote significant differences among the treatments (P < 0.05).

P-8 land and SL. The silt and clay particle contents at 0–20 cm in the three forestlands were significantly higher than in SL. At the depth of 20–40 cm, the silt particle content in P-30 land was significantly greater than that in SL, but there was no significant difference between P-8 land and SL or between P-20 land and SL. The clay particle content in P-20 land was remarkably greater than in SL, but there was no significant difference between P-8 land and SL or between P-30 land and SL. Within the 40–100 cm depth layer, no differences in bulk density or fine particles were observed between the four sample plots (**Table 3**). Additionally, soil pH at 0–100 cm in P-20 land and P-30 land was considerably lower than that in SL, but there was no significant difference between P-8 land and SL within the 60–100 cm depth layer (**Table 3**).

SIC in Shifting Sand Land and Forestlands

Soil inorganic carbon content was enhanced by afforestation. Within the 0–100 cm depth, the SIC content in each 20 cm depth interval in P-8, P-20, and P-30 lands was significantly higher than in SL (**Table 4**). Among the three forestlands, the SIC content increased with plantation age. Within the 0–40 cm layer, the SIC content in P-30 land was considerably higher than in P-20 land, but there was no significant difference between P-20 land and P-8 land. Within the 40–100 cm layer, the SIC content in P-30 land was significantly greater than that in P-20 land, which in turn was greater than that in P-8 land. Afforestation also elevated SIC stocks. The SIC stock at 0–100 cm in SL was 34.2 Mg ha^{-1}, which increased to 42.5, 49.2, and 68.3 Mg ha^{-1} in P-8, P-20 and

TABLE 4 | Soil carbon contents in the four sample plots (g kg^{-1}; mean ± standard deviation; $n = 13$).

Soil carbon	Soil depth (cm)	SL	P-8	P-20	P-30
SIC	0–20	2.18 ± 0.22 Ac	2.77 ± 0.61 Ab	3.17 ± 0.38 Ab	5.24 ± 1.16 Aa
	20–40	2.16 ± 0.19 Ac	2.97 ± 0.27 Ab	3.25 ± 0.58 Ab	4.66 ± 0.77 ABa
	40–60	2.17 ± 0.18 Ad	2.64 ± 0.50 Ac	3.55 ± 0.70 Ab	4.59 ± 0.92 ABa
	60–80	2.19 ± 0.19 Ad	2.67 ± 0.57 Ac	3.21 ± 0.70 Ab	4.55 ± 0.86 ABa
	80–100	2.17 ± 0.20 Ad	2.74 ± 0.33 Ac	3.09 ± 0.58 Ab	3.84 ± 0.58 Ba
SOC	0–20	0.40 ± 0.03 Ad	2.00 ± 0.20 Ac	4.53 ± 0.86 Ab	6.11 ± 1.03 Aa
	20–40	0.38 ± 0.02 Ad	1.54 ± 0.21 Bc	3.88 ± 0.79 Bb	4.98 ± 0.80 Ba
	40–60	0.42 ± 0.04 Ad	1.34 ± 0.21 BCc	3.40 ± 0.59 BCb	4.69 ± 0.77 Ba
	60–80	0.38 ± 0.03 Ad	1.20 ± 0.23 CDc	3.21 ± 0.38 BCb	4.03 ± 0.40 Ca
	80–100	0.40 ± 0.03 Ad	1.03 ± 0.18 Dc	3.00 ± 0.45 Cb	3.43 ± 0.37 Ca

Within each treatment, different uppercase letters denote significant differences among the depths ($P < 0.05$); within each depth, different lowercase letters denote significant differences among the treatments ($P < 0.05$).
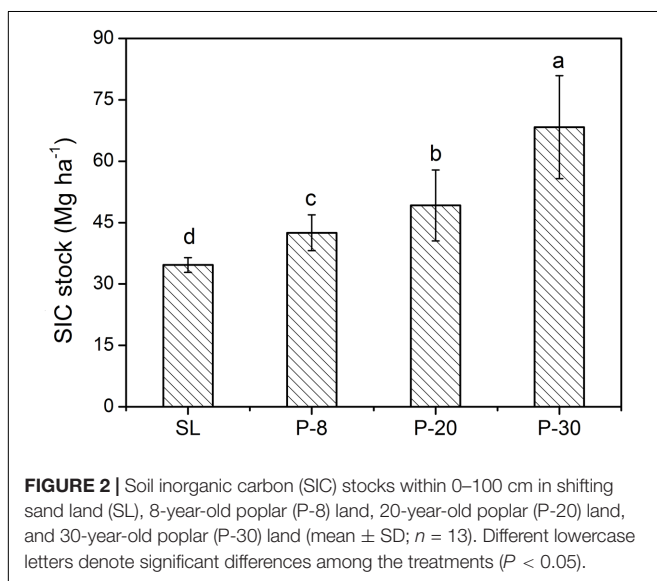

FIGURE 2 | Soil inorganic carbon (SIC) stocks within 0–100 cm in shifting sand land (SL), 8-year-old poplar (P-8) land, 20-year-old poplar (P-20) land, and 30-year-old poplar (P-30) land (mean ± SD; $n = 13$). Different lowercase letters denote significant differences among the treatments ($P < 0.05$).

P-30 lands, respectively (**Figure 2**). The SIC contents in SL, P-8 land and P-20 land were almost evenly distributed among the five 20 cm soil intervals from 0 to 100 cm (**Table 4**). The SIC content in P-30 land at 0–20 cm was significantly higher than at 80–100 cm; however, no differences were observed among the 0–80 cm layers or among the 20–100 cm layers. In addition, the SOC content in the three forestlands was significantly higher in each soil layer than at the same depth in SL (**Table 4**).

δ^{13}C-SIC and δ^{13}C-SOC in Shifting Sand Land and Forestlands

In P-8, P-20, P-30 and SL lands, the δ^{13}C-SIC values showed little vertical variation throughout the 0–100 cm soil layers (**Table 5**). Among the four sample plots, the δ^{13}C-SIC values in SL land were the highest in all five soil layers, and δ^{13}C-SIC value decreased with plantation age after afforestation. At 0–80 cm, the δ^{13}C-SIC values in P-30 land were significantly lower than those in P-20 land, which in turn were lower than those in P-8 land. At 80–100 cm, δ^{13}C-SIC value in P-30 land was also the lowest, but

no difference was observed at this layer between P-20 land and P-8 land. The δ^{13}C-SOC values within the 0–60 cm depth showed a gradual decrease with plantation age after afforestation. At 60–100 cm, the δ^{13}C-SOC values were not significantly different between SL land and P-8 land, but these values in the both plots were dramatically higher than those in P-20 land and P-30 land (**Table 5**).

Figure 3 shows a strong correlation between SIC content and δ^{13}C-SIC. Using all 260 samples, the relationship between δ^{13}C-SIC content and SIC was shown to fit a linear model, and δ^{13}C-SIC was observed to explain more than 70% of the variation in SIC ($R^2 = 0.71$, $P < 0.01$). Our data also showed that the variations in SIC and δ^{13}C-SIC were related to SOC and δ^{13}C-SOC. There was a positive linear relationship ($R^2 = 0.52$, $P < 0.01$) between SOC and SIC content for all soil samples (**Figure 4**). The entire dataset (260 samples) exhibited a positive correlation between δ^{13}C-SOC and δ^{13}C-SIC ($R^2 = 0.63$, $P < 0.01$, **Figure 5**). Additionally, there was no obvious correlation between silt particle content and SIC content (**Figure 6A**) or between clay particle content and SIC content (**Figure 6B**).
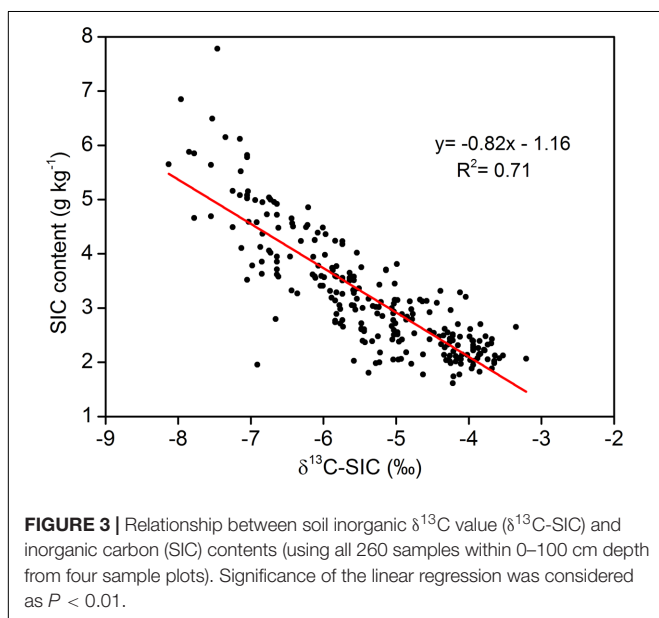
DISCUSSION

SIC Sequestration Following Afforestation and the Contribution of Soil Fine Particles to SIC Sequestration

Our results showed that the SIC stock at depth of 0–100 cm in SL was 34.2 Mg ha^{-1} and that it gradually increased along the chronosequence of afforestation (**Figure 2**). The results were consistent with those reported by Su et al. (2010) and Li Y.Q. et al. (2013), who also observed that SIC increased markedly with plantation age after afforestation on SL. However, our findings were in disagreement with some earlier reports in semiarid regions. In the Columbia Plateau, Oregon, United States, after 10 years, poplar plantations in a desert reduced the SIC concentration from 2.6 to 1.2 g kg^{-1} in the surface layer (Sartori et al., 2007). In the Chinese Loess Plateau, Wang et al.

TABLE 5 | δ^{13}C-SIC and δ^{13}C-SOC in the four sample plots (‰; mean ± standard deviation; $n = 13$).

|	Soil depth (cm)	SL	P-8	P-20	P-30
δ^{13}C-SIC	0–20	−4.08 ± 0.27 Aa	−4.72 ± 0.55 Ab	−5.59 ± 0.65 Ac	−6.72 ± 0.69 Ad
	20–40	−4.04 ± 0.23 Aa	−5.08 ± 0.63 Aa	−5.90 ± 0.47 Ab	−6.41 ± 0.68 Ac
	40–60	−4.00 ± 0.26 Aa	−4.71 ± 0.70 Ab	−5.69 ± 0.51 Ac	−6.55 ± 0.66 Ad
	60–80	−4.05 ± 0.23 Aa	−4.95 ± 0.77 Ab	−5.87 ± 0.63 Ac	−6.69 ± 0.76 Ad
	80–100	−4.06 ± 0.23 Aa	−5.17 ± 0.63 Ab	−5.74 ± 0.62 Ab	−6.58 ± 0.70 Ac
δ^{13}C-SOC	0–20	−18.68 ± 1.54 Aa	−23.36 ± 2.00 Bb	−25.44 ± 1.90 Bb	−27.60 ± 2.20 Bc
	20–40	−18.82 ± 1.66 Aa	−21.46 ± 2.31 ABb	−24.41 ± 1.77 ABc	−26.75 ± 2.28 ABd
	40–60	−19.08 ± 1.89 Aa	−21.60 ± 1.98 ABb	−24.39 ± 1.52 ABc	−25.49 ± 1.47 ABc
	60–80	−19.37 ± 2.06 Aa	−20.84 ± 2.13 Aa	−23.83 ± 1.78 ABb	−25.50 ± 2.30 ABb
	80–100	−18.71 ± 1.81 Aa	−20.34 ± 2.43 Aa	−23.34 ± 1.45 Ab	−24.81 ± 2.42 Ab

Within each treatment, different uppercase letters denote significant differences among the depths (P < 0.05); within each depth, different lowercase letters denote significant differences among the treatments (P < 0.05).

FIGURE 3 | Relationship between soil inorganic δ^{13}C value (δ^{13}C-SIC) and inorganic carbon (SIC) contents (using all 260 samples within 0–100 cm depth from four sample plots). Significance of the linear regression was considered as $P < 0.01$.

$y = -0.82x - 1.16$
$R^2 = 0.71$

FIGURE 4 | Relationship between soil organic carbon (SOC) and inorganic carbon (SIC) contents (using all 260 samples within 0–100 cm depth from four sample plots). Significance of the linear regression was considered as $P < 0.01$.

$y = 0.49x + 2.11$
$R^2 = 0.52$

(2016) reported that the SIC storage at depth of 0–100 cm in the farmland was significantly lower than that in the restored artificial forestland, with a difference of 16.8 Mg ha^{-1}. The SIC reduction in these inconsistent findings was mainly caused by irrigation or surface runoff, which can remove mass containing dissolved inorganic carbon. In the present study, similar processes would not be applicable because there was no irrigation or heavy rainfall. Therefore, our findings indicate that afforestation on shifting SL has a high potential to sequester SIC in degraded semiarid regions.
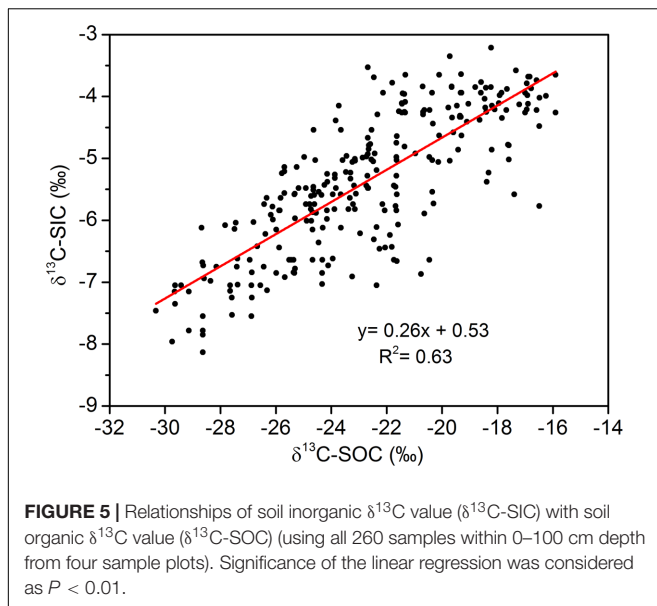
One theory posits that soil fine particles may play an important role in SIC sequestration following afforestation (Li et al., 2012). Plant canopies can intercept and deposit fine particles from the wind-sand flow after afforestation. This sediment contains rich carbonate sources, such as calcite, and causes a rapid SIC accumulation in surface soil (0–20 cm) (Wang et al., 2006). However, we found that this theory could not provide a complete explanation for SIC accumulation. Afforestation on SL not only
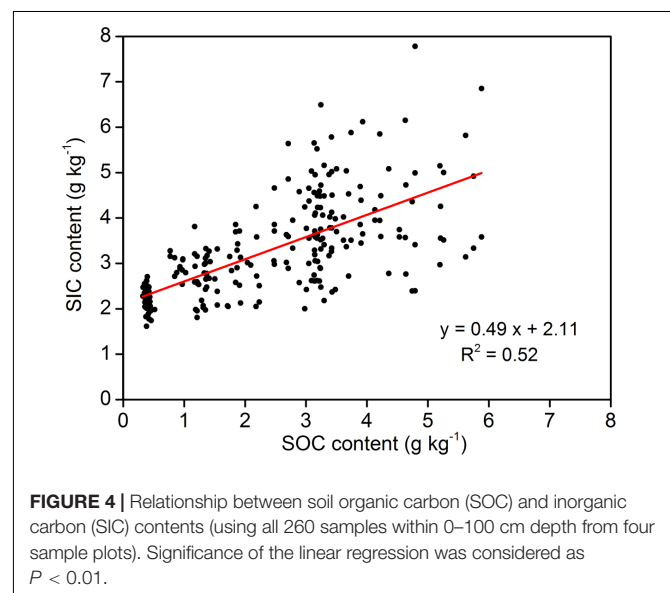
elevates SIC stock in the surface soil layer, but also increases SIC levels in the deeper layers (**Table 4**; Li Y.Q. et al., 2013). Nevertheless, afforestation enhanced fine particles only at a depth of 0–40 cm, but not in the 40–100 cm depths (**Table 3**). In the deep layers (>40 cm), soil fine particles stack at an exceptionally slow rate and contribute little to SIC sequestration (Li et al., 2007). Moreover, we detected no correlation between fine particles and SIC content in the present study (**Figure 6**), further suggesting that the contribution of soil fine particles by the canopy to SIC sequestration is limited for the 0–100 cm soil layer. This phenomenon indicates that SIC sequestration is not exclusively derived from fine particle deposition and that other SIC accumulation processes may be occurring after afforestation.

Effects of Afforestation on Stable Carbon Isotopes and Implications for Revealing the Mechanism of SIC Sequestration

We found that δ^{13}C-SIC decreased with plantation age in forestlands (**Table 5**). Wang J.P. et al. (2015) found that the

FIGURE 5 | Relationships of soil inorganic δ^{13}C value (δ^{13}C-SIC) with soil organic δ^{13}C value (δ^{13}C-SOC) (using all 260 samples within 0–100 cm depth from four sample plots). Significance of the linear regression was considered as $P < 0.01$.
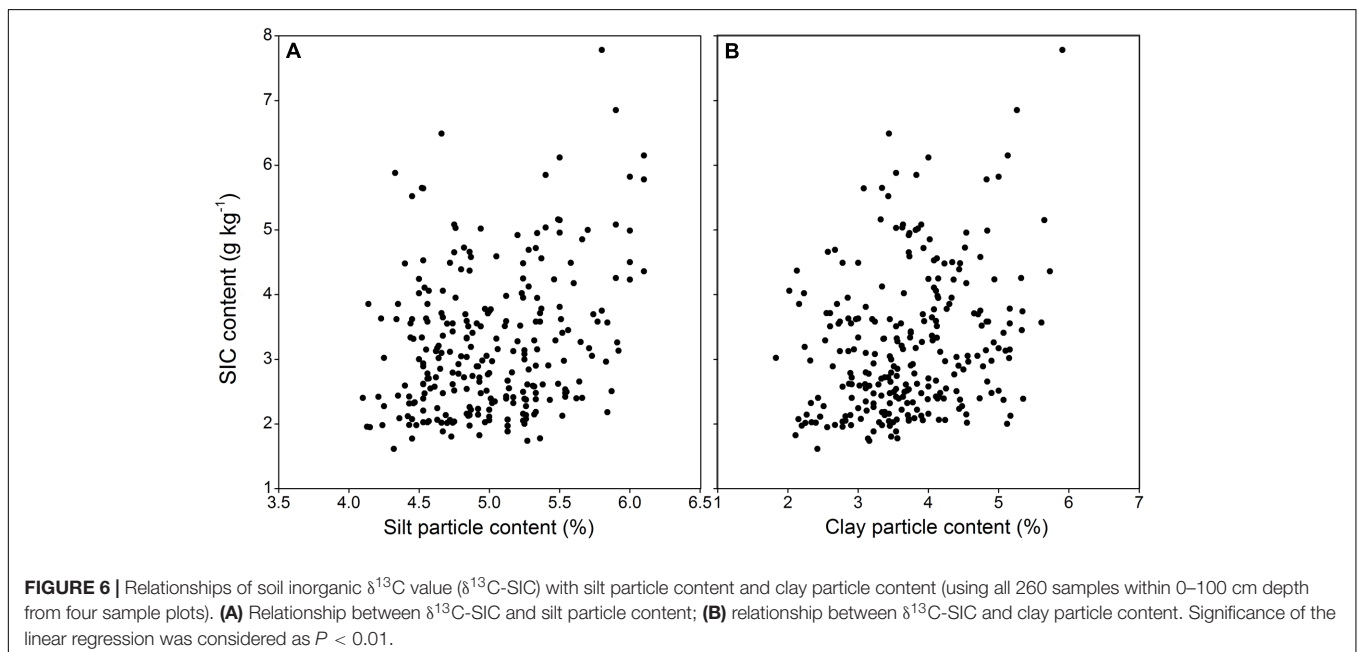
δ^{13}C-SIC for desert soil was significantly higher than that for shrubland soil on the northeastern edge of the Taklamakan Desert, China. Liu et al. (2014) also pointed out that the δ^{13}C value of soil carbonate along a chronosequence decreased gradually with vegetation restoration. SIC is composed of the LIC and PIC, which have distinct δ^{13}C-SIC values. The changes in δ^{13}C-SIC following vegetation rehabilitation can be used to explain the reason for SIC variation (Stevenson et al., 2005). There is sufficient evidence that the decrease in δ^{13}C-SIC indicates PIC formation when land use patterns change (Jin et al., 2014; Liu et al., 2014; Wang et al., 2014, 2016; Wang J.P. et al., 2015; Bughio et al., 2016). Accordingly,

the decrease in δ^{13}C-SIC with plantation age in our study indicates that afforestation induced abundant PIC formation. Furthermore, a strong negative linear relationship between δ^{13}C-SIC and SIC content in our study (**Figure 3**), which was also observed by Wang X.J. et al. (2015) in the northwest China, suggests that a decreasing δ^{13}C-SIC is associated with SIC sequestration following afforestation. Specifically, PIC formation is accompanied by SIC sequestration, as the decrease in δ^{13}C-SIC is indicative of the formation of PIC. Therefore, the carbon isotope data in this study indicate that SIC sequestration is probably caused by PIC formation after afforestation on SL. Additionally, an estimation of the amount of PIC would be very important to better understanding the contribution of PIC to SIC sequestration. Based on the precise δ^{13}C-SIC, δ^{13}C-PIC and δ^{13}C-LIC values and empirical formulas, Wang et al. (2014) successfully estimated the accumulation rate of PIC under fertilization for loess soil. This method can ostensibly be used to calculate the amount of PIC in the forestlands in our study. However, an accurate δ^{13}C-LIC value in the desert cannot be measured with the current technology, so we cannot supply values for the PIC stocks in this study. The δ^{13}C-LIC of desert soil should be precisely identified in future studies because it is crucial for quantifying PIC stock.

Effect of SOC Accumulation on PIC Formation

In this study, afforestation simultaneously enhanced SIC and SOC contents (**Figure 2**), and SIC content was positively correlated with SOC content (**Figure 4**). Similar relationships have also been identified in other arid and semiarid regions in China (Zhang N. et al., 2010; Wang X.J. et al., 2015; Guo et al., 2016). These results suggest that the increase of SIC following

FIGURE 6 | Relationships of soil inorganic δ^{13}C value (δ^{13}C-SIC) with silt particle content and clay particle content (using all 260 samples within 0–100 cm depth from four sample plots). **(A)** Relationship between δ^{13}C-SIC and silt particle content; **(B)** relationship between δ^{13}C-SIC and clay particle content. Significance of the linear regression was considered as $P < 0.01$.

afforestation may be related to SOC accumulation. Furthermore, our results showed that there was a decrease in both δ^{13}C-SIC and δ^{13}C-SOC with plantation age. δ^{13}C-SIC was strongly positively correlated with δ^{13}C-SOC (**Figure 5**), a finding that is consistent with the observations of Landi et al. (2003). In other words, the decrease in δ^{13}C-SIC was accompanied by a decrease in δ^{13}C-SOC. The decrease in δ^{13}C-SIC indicates PIC formation, and SOC accumulation invariably leads to a decrease in δ^{13}C-SOC due to plant litter input (Trolier et al., 1996; Jin et al., 2014). These results further imply that the PIC formation following afforestation is correlated with SOC accumulation. Soil organic matter affected PIC formation by regulating soil CO_2 concentration and the precipitation of carbonate in the alkaline environment (Monger et al., 2015). PIC accumulation involves two main reactions:

$$2CO_2 + 2H_2O \leftrightarrow 2HCO_3^- + 2H^+ \tag{3}$$

$$Ca^{2+} + 2HCO_3^- \leftrightarrow CaCO_3 + H_2O + CO_2 \tag{4}$$
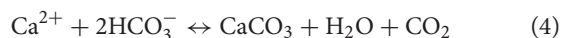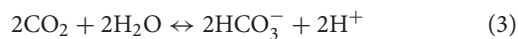
A mass of CO_2 is released into the soil following shrub and tree plantation in deserts, mainly due to the decomposition of the increased amount of organic matter (Zhang Z.S. et al., 2013). In general, an increase in soil CO_2 concentration would lead to the production of HCO_3^-. The accumulated HCO_3^- can drive reaction (4) to the right, resulting in the precipitation of carbonate (Wang X.J. et al., 2015; Zamanian et al., 2016). When 2 mole of CO_2 is consumed, 1 mole of $CaCO_3$ is generated. At our study site, the soil has a pH greater than 8 (**Table 3**) and is rich in available Ca^{2+} and Mg^{2+} (**Table 1**). The decomposition of the increased SOC in forestlands would dramatically elevate the soil CO_2 concentration and facilitate the occurrence of reaction (3). The alkaline environmental conditions could neutralize the H^+ from reaction (3), which may be the reason for the decline in pH in forestlands (**Table 3**). These conditions also continuously promote the formation of HCO_3^-. The newly generated HCO_3^- combined with available cations may cause PIC accumulation following afforestation (Meyer et al., 2014; Monger et al., 2015). In addition to the CO_2 emitted via decomposition of the increased SOC, soil CO_2 respired by the roots of poplar trees (autotrophic respiration) would affect the formation of PIC. The effects of autotrophic respiration on PIC formation in plantation lands need to be studied in future. Additionally, a long-term study by observing SIC, SOC, soil carbon isotopes, soil CO_2 concentration and available cations in the same forestland is required, which could more directly and precisely characterize

the mechanisms of SIC variation along a chronosequence of afforestation.

CONCLUSION

Our data demonstrate that afforestation on shifting SL has a high potential to sequester SIC in degraded semiarid regions. Afforestation elevated soil fine particles only at 0–40 cm, and there was no correlation between SIC content and soil fine particles, suggesting that the contribution of soil fine particle deposition to SIC accumulation is limited. The decrease in δ^{13}C-SIC along a chronosequence of forestland and the relationship between δ^{13}C-SIC and SIC content both indicate that SIC sequestration following afforestation is probably caused by PIC formation. The positive correlations between SIC content and SOC content and between δ^{13}C-SIC and δ^{13}C-SOC imply that the newly formed PIC may be closely related to SOC accumulation. Our findings suggest that SIC plays an important role in the carbon cycle in semiarid areas and that by overlooking SIC, we may substantially underestimate carbon sequestration capacities following vegetation rehabilitation. Our stable carbon isotope data will help to form an understanding of the mechanisms of SIC formation and transformation in arid and semiarid areas.

AUTHOR CONTRIBUTIONS

JL designed the experiment; YG, JT, and YP carried out the field work; YG and JL analyzed the data; YG wrote the manuscript; and JL assisted with revising the draft manuscript.

REFERENCES

Bughio, M. A., Wang, P. L., Meng, F. Q., Qing, C., Kuzyakov, Y., Wang, X. J., et al. (2016). Neoformation of pedogenic carbonates by irrigation and fertilization and their contribution to carbon sequestration in soil. *Geoderma* 262, 12–19. doi: 10.1016/j.geoderma.2015.08.003

Cerling, T. E., Quade, J., Wang, Y., and Bowman, J. R. (1989). Carbon isotopes in soils and palaeosols as ecology and palaeoecology indicators. *Nature* 341, 138–139. doi: 10.1038/341138a0

Chang, R. Y., Fu, B. J., Liu, G. B., Wang, S., and Yao, X. L. (2012). The effects of afforestation on soil organic and inorganic carbon: a case study of

the Loess Plateau of China. *Catena* 95, 145–152. doi: 10.1016/j.catena.2012.02.012

Coplen, T. B. (2011). Guidelines and recommended terms for expression of stable-isotope-ratio and gas-ratio measurement results. *Rapid Commun. Mass Spectrom.* 25, 2538–2560. doi: 10.1002/rcm.5129

Delgado-Baquerizo, M., Maestre, F. T., Gallardo, A., Bowker, M. A., Wallenstein, M. D., Quero, J. L., et al. (2013). Decoupling of soil nutrient cycles as a function of aridity in global drylands. *Nature* 502, 672–676. doi: 10.1038/nature12670

Deng, L., Liu, G. B., and Shangguan, Z. P. (2014). Land-use conversion and changing soil carbon stocks in China's "Grain-for-Green" program: a synthesis. *Global Change Biol.* 20, 3544–3556. doi: 10.1111/gcb.12508

Farley, K. A., Kelly, E. F., and Hofstede, R. G. M. (2004). Soil organic carbon and water retention after conversion of grasslands to pine plantations in the Ecuadorian Andes. *Ecosystems* 7, 729–739. doi: 10.1007/s10021-004-0047-5

Gao, G. L., Ding, G. D., Zhao, Y. Y., Wu, B., Zhang, Y. Q., Qin, S. G., et al. (2014). Fractal approach to estimating changes in soil properties following the establishment of *Caragana korshinskii* shelterbelts in Ningxia, NW China. *Ecol. Indic.* 43, 236–243. doi: 10.1016/j.ecolind.2014.03.001

Guo, Y., Wang, X. J., Li, X. L., Wang, J. P., Xu, M. G., and Li, D. W. (2016). Dynamics of soil organic and inorganic carbon in the cropland of upper Yellow River Delta, China. *Sci. Rep.* 6:36105. doi: 10.1038/srep36105

Huang, G., Zhao, X. Y., Li, Y. Q., and Cui, J. Y. (2012). Restoration of shrub communities elevates organic carbon in arid soils of northwestern China. *Soil Biol. Biochem.* 47, 123–132. doi: 10.1016/j.soilbio.2011.12.025

Jackson, R. B., Banner, J. L., Jobbágy, E. G., Pockman, W. T., and Wall, D. H. (2002). Ecosystem carbon loss with woody plant invasion of grasslands. *Nature* 418, 623–626. doi: 10.1038/nature00910

Jin, Z., Dong, Y. S., Wang, Y. Q., Wei, X. R., Wang, Y. F., Cui, B. L., et al. (2014). Natural vegetation restoration is more beneficial to soil surface organic and inorganic carbon sequestration than tree plantation on the Loess Plateau of China. *Sci. Total Environ.* 48, 615–623. doi: 10.1016/j.scitotenv.2014.03.105

Jobbágy, E. G., and Jackson, R. B. (2003). Patterns and mechanisms of soil acidification in the conversion of grasslands to forests. *Biogeochemistry* 64, 205–229. doi: 10.1023/A:1024985629259

Lal, R. (2004). Soil carbon sequestration impacts on global climate change and food security. *Science* 304, 1623–1627. doi: 10.1126/science.1097396

Lal, R. (2009). Sequestering carbon in soils of arid ecosystems. *Land Degrad. Dev.* 20, 441–454. doi: 10.1002/ldr.934

Lal, R. (2010). Managing soils and ecosystems for mitigating anthropogenic carbon emissions and advancing global food security. *Bioscience* 60, 708–721. doi: 10.1525/bio.2010.60.9.8

Landi, A., Mermut, A. R., and Anderson, D. W. (2003). Origin and rate of pedogenic carbonate accumulation in Saskatchewan soils, Canada. *Geoderma* 117, 143–156. doi: 10.1016/S0016-7061(03)00161-7

Li, C. F., Zhang, C., Luo, G. P., Chen, X., Maisupova, B., Madaminov, A. A., et al. (2015). Carbon stock and its responses to climate change in Central Asia. *Glob. Change Biol.* 21, 1951–1967. doi: 10.1111/gcb.12846

Li, G. J., Chen, J., and Chen, Y. (2013). Primary and secondary carbonate in Chinese loess discriminated by trace element composition. *Geochim. Cosmochim. Acta* 103, 26–35. doi: 10.1016/j.gca.2012.10.049

Li, X. J., Li, X. R., Wang, X. P., and Yang, H. T. (2016). Changes in soil organic carbon fractions after afforestation with xerophytic shrubs in the Tengger Desert, northern China. *Eur. J. Soil Sci.* 67, 184–195. doi: 10.1111/ejss.12315

Li, X. R., Kong, D. S., Tan, H. J., and Wang, X. P. (2007). Changes in soil and vegetation following stabilisation of dunes in the southeastern fringe of the Tengger Desert, China. *Plant Soil* 300, 221–231. doi: 10.1007/s11104-007-9407-1

Li, Y. Q., Awada, T., Zhou, X. H., Shang, W., Chen, Y. P., Zuo, X. A., et al. (2012). Mongolian pine plantations enhance soil physico-chemical properties and carbon and nitrogen capacities in semi-arid degraded sandy land in China. *Appl. Soil Ecol.* 56, 1–9. doi: 10.1016/j.apsoil.2012.01.007

Li, Y. Q., Brandle, J., Awada, T., Chen, Y. P., Han, J. J., Zhang, F. X., et al. (2013). Accumulation of carbon and nitrogen in the plant–soil system after afforestation of active sand dunes in China's Horqin Sandy Land. *Agric. Ecosyst. Environ.* 177, 75–84. doi: 10.1016/j.agee.2013.06.007

Liu, R. T., Zhao, H. L., and Zhao, X. Y. (2013). Changes in soil macrofaunal community composition under selective afforestation in shifting sand lands in Horqin of Inner Mongolia, northern China. *Ecol. Res.* 28, 1–8. doi: 10.1007/s11284-012-0982-0

Liu, W. G., Wei, J., Cheng, J. M., and Li, W. J. (2014). Profile distribution of soil inorganic carbon along a chronosequence of grassland restoration on a 22-year scale in the Chinese Loess Plateau. *Catena* 121, 321–329. doi: 10.1016/j.catena.2014.05.019

Meyer, N. A., Breecker, D. O., Young, M. H., and Litvak, M. E. (2014). Simulating the effect of vegetation in formation of pedogenic carbonate. *Soil Sci. Soc. Am. J.* 78, 914–924. doi: 10.2136/sssaj2013.08.0326

Mi, N., Wang, S. Q., Liu, J. Y., Yu, G. R., Zhang, W. J., and Jobbágy, E. (2008). Soil inorganic carbon storage pattern in China. *Glob. Chang. Biol.* 14, 2380–2387. doi: 10.1111/j.1365-2486.2008.01642.x

Mielnick, P., Dugas, W. A., Mitchell, K., and Havstad, K. (2005). Long-term measurements of CO2 flux and evapotranspiration in a Chihuahuan desert grassland. *J. Arid. Environ.* 60, 423–436. doi: 10.1016/j.jaridenv.2004.06.001

Monger, H. C., Kraimer, R. A., Khresat, S., Cole, D. R., Wang, X. J., and Wang, J. P. (2015). Sequestration of inorganic carbon in soil and groundwater. *Geology* 43, 375–378. doi: 10.1130/G36449.1

Qiu, L., Wei, X., Gao, J., and Zhang, X. (2015). Dynamics of soil aggregate-associated organic carbon along an afforestation chronosequence. *Plant Soil* 391, 237–251. doi: 10.1007/s11104-015-2415-7

Rao, Z. G., Zhu, Z. Y., Chen, F. H., and Zhang, J. W. (2006). Does δ13Ccarb of the Chinese loess indicate past C3/C4 abundance? A review of research on stable carbon isotopes of the Chinese loess. *Quat. Sci. Rev.* 25, 2251–2257. doi: 10.1016/j.quascirev.2006.03.013

Reynolds, J. F., Smith, D. M. S., Lambin, E. F., Turner, B. L. II, Mortimore, M., Batterbury, S. P. J., et al. (2007). Global desertification: building a science for dryland development. *Science* 316, 847–851. doi: 10.1126/science.1131634

Sartori, F., Lal, R., Ebinger, M. H., and Eaton, J. A. (2007). Changes in soil carbon and nutrient pools along a chronosequence of poplar plantations in the Columbia Plateau, Oregon, USA. *Agric. Ecosyst. Environ.* 122, 325–339. doi: 10.1016/j.agee.2007.01.026

Schlesinger, W. H. (1982). Carbon storage in the Caliche of arid soils: a case study from Arizona. *Soil Sci.* 133, 247–255. doi: 10.1097/00010694-198204000-00008

Stevenson, B. A., Kelly, E. F., McDonald, E. V., and Busacca, A. J. (2005). The stable carbon isotope composition of soil organic carbon and pedogenic carbonates along a bioclimatic gradient in the Palouse region, Washington State, USA. *Geoderma* 124, 37–47. doi: 10.1016/j.geoderma.2004.03.006

Su, Y. Z., Wang, X. F., Yang, R., and Lee, J. (2010). Effects of sandy desertified land rehabilitation on soil carbon sequestration and aggregation in an arid region in China. *J. Environ. Manage.* 91, 2109–2116. doi: 10.1016/j.jenvman.2009.12.014

Su, Y. Z., and Zhao, H. L. (2003). Soil properties and plant species in an age sequence of *Caragana microphylla* plantations in the Horqin Sandy Land, north China. *Ecol. Eng.* 20, 223–235. doi: 10.1016/S0925-8574(03)00042-9

Tan, W. F., Zhang, R., Cao, H., Huang, C. Q., Yang, Q. K., Wang, M. K., et al. (2014). Soil inorganic carbon stock under different soil types and land uses on the Loess Plateau region of China. *Catena* 121, 22–30. doi: 10.1016/j.catena.2014.04.014

Trolier, M., White, J. W. C., Tans, P. P., Masarie, K. A., and Gemery, P. A. (1996). Monitoring the isotopic composition of atmospheric CO2: measurements from the NOAA global air sampling network. *J. Geophys. Res.* 101, 25897–25916. doi: 10.1029/96JD02363

Walkley, A., and Black, I. A. (1934). An examination of the Degtjareff method for determining soil organic matter and a proposed modification of the chromic acid titration method. *Soil Sci.* 37, 29–38. doi: 10.1097/00010694-193401000-00003

Wang, J. P., Monger, C., Wang, X. J., Serena, M., and Leinauer, B. (2016). Carbon sequestration in response to grassland–shrubland–turfgrass conversions and a test for carbonate biomineralization in desert soils, New Mexico, USA. *Soil Sci. Soc. Am. J.* 80, 1591–1603. doi: 10.2136/sssaj2016.03.0061

Wang, J. P., Wang, X. J., Zhang, J., and Zhao, C. Y. (2015). Soil organic and inorganic carbon and stable carbon isotopes in the Yanqi Basin of northwestern China. *Eur. J. Soil Sci.* 66, 95–103. doi: 10.1111/ejss.12188

Wang, X. J., Wang, J. P., Xu, M. G., Zhang, W. J., Fan, T. L., and Zhang, J. (2015). Carbon accumulation in arid croplands of northwest China: pedogenic carbonate exceeding organic carbon. *Sci. Rep.* 5:11439. doi: 10.1038/srep11439

Wang, X. J., Wang, J. P., and Zhang, J. (2012). Comparisons of three methods for organic and inorganic carbon in calcareous soils of Northwestern China. *PLoS ONE* 7:e44334. doi: 10.1371/journal.pone.0044334

Wang, X. J., Xu, M. G., Wang, J. P., Zhang, W. J., Yang, X. Y., Huang, S. M., et al. (2014). Fertilization enhancing carbon sequestration as carbonate in arid cropland: assessments of long-term experiments in northern China. *Plant Soil* 380, 89–100. doi: 10.1007/s11104-014-2077-x

Wang, X. P., Li, X. R., Xiao, H. L., and Pan, Y. X. (2006). Evolutionary characteristics of the artificially revegetated shrub ecosystem in the Tengger Desert, northern China. *Ecol. Res.* 21, 415–424. doi: 10.1007/s11284-005-0135-9

Wang, Y. G., Li, Y., Ye, X. H., Chu, Y., and Wang, X. P. (2010). Profile storage of organic/inorganic carbon in soil: from forest to desert. *Sci. Total Environ.* 408, 1925–1931. doi: 10.1016/j.scitotenv.2010.01.015

Zamanian, K., Pustovoytov, K., and Kuzyakov, Y. (2016). Pedogenic carbonates: Forms and formation processes. *Earth Sci. Rev.* 157, 1–17. doi: 10.1016/j.earscirev.2016.03.003

Zhang, F., Wang, X. J., Guo, T. W., Zhang, P. L., and Wang, J. P. (2015). Soil organic and inorganic carbon in the loess profiles of Lanzhou area: implications of deep soils. *Catena* 126, 68–74. doi: 10.1016/j.catena.2014.10.031

Zhang, K., Dang, H., Tan, S., Cheng, X., and Zhang, Q. (2010). Change in soil organic carbon following the 'Grain-For-Green' programme in China. *Land Degrad. Dev.* 21, 13–23. doi: 10.1002/ldr.954

Zhang, N., He, X. D., Gao, Y. B., Li, Y. H., Wang, H. T., Ma, D., et al. (2010). Pedogenic carbonate and soil dehydrogenase activity in response to soil organic matter in *Artemisia ordosica* community. *Pedosphere* 20, 229–235. doi: 10.1016/S1002-0160(10)60010-0

Zhang, Y., Cao, C. Y., Han, X. S., and Jiang, S. Y. (2013). Soil nutrient and microbiological property recoveries via native shrub and semi-shrub plantations on moving sand dunes in Northeast China. *Ecol. Eng.* 53, 1–5. doi: 10.1016/j.ecoleng.2013.01.012

Zhang, Z. S., Li, X. R., Nowak, R. S., Wu, P., Gao, Y. H., Zhao, Y., et al. (2013). Effect of sand-stabilizing shrubs on soil respiration in a temperate desert. *Plant Soil* 367, 449–463. doi: 10.1007/s11104-012-1465-3